oceans

MDPI

Article

Influence of Inorganic Nutrients on a North Atlantic Microbial Community's Response to Ocean Alkalinity Enhancement

Inês de Castro [1,*], Susana C. Ribeiro [2], António Louvado [3], Newton Carlos Marcial Gomes [3], Mário Cachão [4,5], Paulo F. Silva Borges [1], Eduardo Brito de Azevedo [1] and Joana Barcelos e Ramos [1]

[1] Group of Climate, Meteorology and Global Change, IITAA—Institute of Agricultural and Environmental Research and Technology, University of the Azores, 9700-042 Angra do Heroísmo, Portugal
[2] Group of Food Science and Health, IITA—Institute of Agricultural and Environmental Research and Technology, University of the Azores, 9700-042 Angra do Heroísmo, Portugal
[3] Centre for Environmental and Marine Studies (CESAM), Department of Biology, University of Aveiro, Campus Universitário de Santiago, 3810-193 Aveiro, Portugal
[4] Instituto D. Luiz (IDL), Faculty of Sciences, University of Lisbon, Campo Grande Edifício C1, Piso 1, 1749-016 Lisbon, Portugal
[5] Department of Geology, Faculty of Sciences, University of Lisbon, 1749-016 Lisbon, Portugal
* Correspondence: inesmcastro@ua.pt

Abstract

Ocean Alkalinity Enhancement (OAE) is a promising carbon dioxide removal strategy, but its ecological impacts on marine microbial communities under varying nutrient conditions remain poorly understood. We conducted laboratory incubations using a natural North Atlantic microbial assemblage to investigate the response to OAE under both natural and nutrient-enriched regimes. We tracked phytoplankton and bacterioplankton dynamics, biomass, and leucine aminopeptidase (LAP) and alkaline phosphatase (ALP) activity as indicators of organic matter remineralization. OAE consistently reduced phytoplankton abundance in both nutrient regimes, potentially due to CO_2 limitation, resulting in lower production of phytoplankton-derived organic matter. This reduction was reflected in decreased LAP activity and shifts in the relative abundance of phytoplankton-associated bacterial taxa. These findings indicate that OAE can directly affect phytoplankton through carbonate chemistry alterations, with potential microbial responses largely mediated by changes in organic matter availability. While short-term microbial disruptions were modest, the ecological consequences of altered bloom dynamics should be carefully considered in future OAE deployment strategies.

Keywords: ocean alkalinity enhancement; marine microbial communities; nutrient limitation; extracellular enzyme activity

Academic Editor: Diego Macías

Received: 6 June 2025
Revised: 12 September 2025
Accepted: 23 September 2025
Published: 9 October 2025

Citation: de Castro, I.; Ribeiro, S.C.; Louvado, A.; Gomes, N.C.M.; Cachão, M.; Silva Borges, P.F.; Brito de Azevedo, E.; Barcelos e Ramos, J. Influence of Inorganic Nutrients on a North Atlantic Microbial Community's Response to Ocean Alkalinity Enhancement. *Oceans* **2025**, *6*, 65. https://doi.org/10.3390/oceans6040065

1. Introduction

Mitigation of climate change is urgent, particularly to meet the targets set by the Paris Agreement, which aims to limit global warming to below 2 °C (ideally 1.5 °C) [1]. To achieve this goal, global emissions must peak before 2025 and fall by 43% by 2030 [2]. Current emission trajectories, however, remain incompatible with these targets, posing severe risks to ocean health. As a result, ocean-based carbon dioxide removal (mCDR) strategies are gaining momentum [3,4].

Ocean Alkalinity Enhancement (OAE) is a mCDR approach that enhances the ocean's natural capacity to sequester atmospheric CO_2 by increasing alkalinity and thereby shifting the carbonate equilibrium toward bicarbonate (HCO_3^-) and carbonate (CO_3^{2-}) ion

formation [5–9]. Alkalinity can be enhanced through the addition of natural minerals (e.g., silicates, carbonates) or synthetic compounds like quicklime (CaO) and slaked lime ($Ca(OH)_2$). Among these, CaO addition, often referred to as "ocean liming", when non-CO_2-equilibrated, offers rapid alkalinity enhancement while simultaneously helping to counteract ocean acidification by increasing seawater pH [5,10–12]. However, it also raises concerns regarding energy demands and CO_2 emissions associated with its production [13–15].

Although research on the ecological impacts of OAE is expanding, most studies have focused on carbonate-based, CO_2-equilibrated scenarios. This includes recent mesocosm experiments in the subtropical North Atlantic, which have reported generally limited effects on phytoplankton physiology, microbial activity, and biogeochemical fluxes under these conditions [16–19]. Other efforts have tested more realistic deployment scenarios using steel slag, a CaO-rich byproduct of industrial processes, to assess both biogeochemical impacts and potential trace metal release [20,21]. While these studies provide valuable findings, they have largely emphasized phytoplankton responses and primary production [22,23] with less attention given to bacterioplankton dynamics, which play a crucial role in organic matter turnover and nutrient regeneration.

This microbial interface, where phytoplankton-derived organic matter fuels heterotrophic bacterial activity, is key to understanding how OAE may influence carbon export efficiency and nutrient cycling. Importantly, environmental context matters: insights from ocean acidification studies indicate that nutrient availability, particularly phosphate, can modulate microbial responses [24–26]. This is especially relevant in oligotrophic systems like the subtropical North Atlantic, where seasonal or episodic nutrient pulses regulate microbial productivity and remineralization [24]. Furthermore, timing may be critical when deploying OAE, as ecological outcomes can vary significantly between nutrient-depleted and nutrient-replete periods [27]. In nutrient-depleted conditions, microbial responses may differ in ways that affect both ecosystem function and the efficiency of carbon removal. Finally, interactions with artificial upwelling, a proposed complementary CDR strategy, could further influence microbial and biogeochemical dynamics [28]. Testing OAE under varying nutrient conditions can therefore help determine optimal deployment timing and assess its potential compatibility with artificial upwelling.

In this study, we conducted a laboratory incubation with a natural marine microbial community from the North Atlantic to evaluate the combined effects of CaO-based OAE and nutrient availability on microbial ecosystem dynamics. We examined changes in phytoplankton and bacterioplankton community composition and biomass under ambient and nutrient-enriched conditions, along with the activities of two key extracellular enzymes—leucine aminopeptidase (LAP) and alkaline phosphatase (ALP)—to assess microbial functional responses. These two enzymes were selected because they serve as markers of microbial nutrient cycling: LAP reflects organic nitrogen degradation, while ALP activity is commonly induced under phosphate limitation. Our aim was to determine how microbial ecosystems respond to OAE under contrasting nutrient conditions and to explore how baseline nutrient availability may shape the ecological outcomes of OAE deployment.

2. Materials and Methods

2.1. Sampling Site

The effects of OAE under different nutrient settings were assessed on a natural microbial marine community from the North Atlantic, offshore Terceira Island (38°39′20.3″ N, 27°16′54.3″ W), in the Azores on May 2022. Nutrient concentrations at Negrito Bay were assessed along a shore-to-offshore transect to characterize baseline variability (see Figure 1, Supplementary Figure S1).

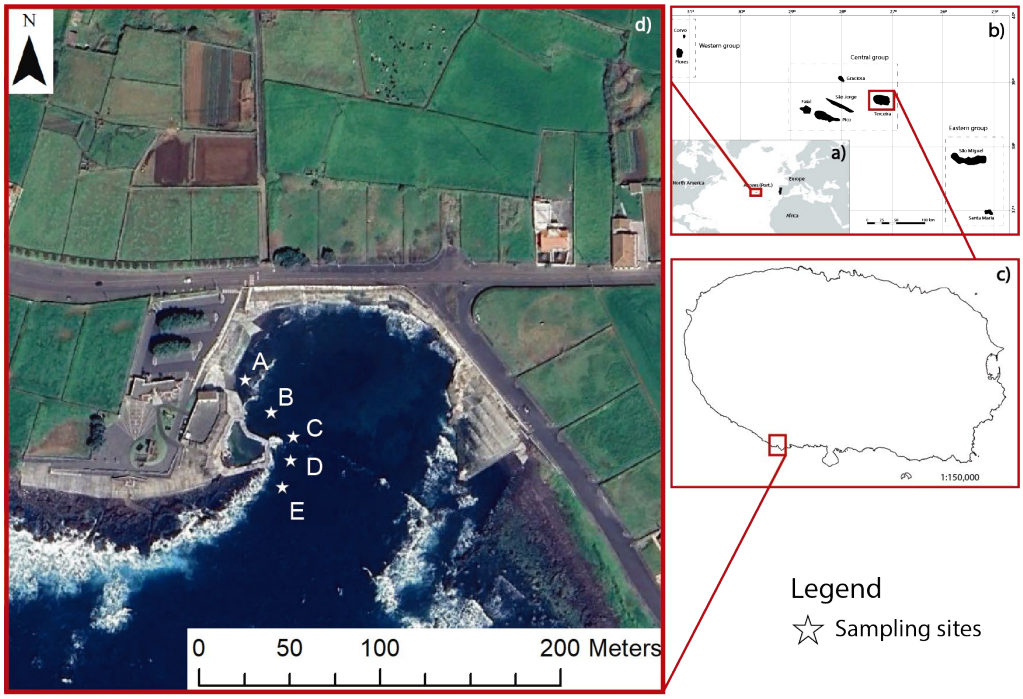

Figure 1. Map of the sampling area, including five sampling sites at the Negrito Bay, Angra do Heroísmo. (**a**) Azores Archipelago location; (**b**) Azores Archipelago and Terceira Island location; (**c**) study location in Terceira Island; (**d**) Negrito bay, the sampling site, and the transect from A to E (Spatial data were projected using the WGS84 geodetic datum).

2.2. Experimental Setup

The seawater collected was immediately filtered through a 200 µm mesh on site, to exclude zooplankton and debris, as our focus did not include higher trophic levels. At the lab, the community was divided into two containers, one corresponding to the natural nutrient treatment (NN) and another corresponding to the enhanced nutrient treatment (EN). Specifically, in the NN, no nutrients were added, while in the EN, nitrate and phosphate were added at the final concentrations of 80.77 and 3.48 µM, respectively, to prevent nutrient limitation during the exponential growth phase and ensure that any potential depletion would occur only in the later stages of the experiment. Silicate was not added, as ambient concentrations in Negrito Bay were already high (47.81 µM; Supplementary Figure S1), and previous experiments in this system indicated that silicate limitation was unlikely under the conditions tested. Initial measurements at t0 confirmed the effectiveness of the nutrient manipulation, with the EN treatment reaching target nitrate and phosphate concentrations (Table 1), while the NN treatment reflected background levels typical of Negrito Bay (see Figure 2). Nutrient regimes were based on a shore-to-offshore transect at Negrito Bay (Figure 1), which showed modest spatial variability but elevated baseline nutrient levels (e.g., 7.91 µM NO_3^-, 0.24 µM PO_4^{3-}, 47.81 µM $Si(OH)_4$; Supplementary Figure S1).

Table 1. Inorganic nutrient starting conditions under the two nutrient treatments: natural (NN) and enhanced (EN).

Nutrient Condition	NO_3^- (µM)	PO_4^{3-} (µM)	$Si(OH)_4$ (µM)	NO_2^- (µM)
NN	7.91	0.24	47.81	0.31
EN	80.77	3.48	44.38	0.17

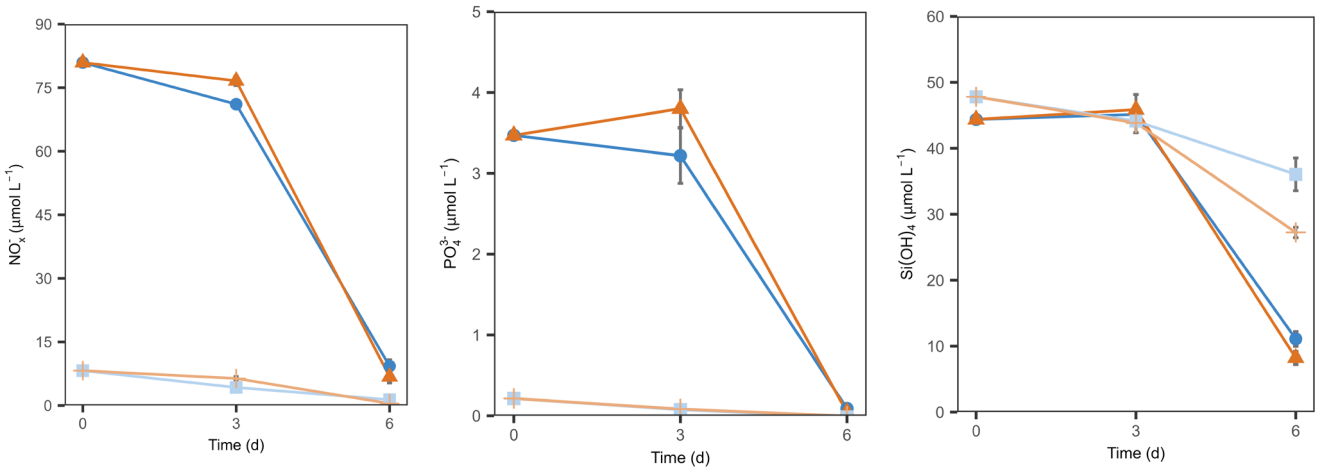

Figure 2. Temporal development of inorganic nutrient concentrations of: (**a**) nitrate + nitrite; (**b**) phosphate; (**c**) silicate. Line colors indicate alkalinity conditions (orange = ambient, blue = OAE). Line shading reflects nutrient treatment (lighter = natural nutrients (NN), darker = enhanced nutrients (EN)). Symbols denote conditions: plus = ambient NN, triangles = ambient EN, squares = OAE NN, and circles = OAE EN.

The EN treatment was designed to simulate nutrient-replete conditions, with the objective of isolating the biological effects of ocean alkalinity enhancement (OAE) from those caused by nutrient limitation.

Subsequently, from each nutrient treatment, half of the containers obtained were further manipulated by increasing total alkalinity (TA) by 250 µmol kg^{-1} using CaO (Calcidrata, Portugal). This value was chosen because it has previously been reported to ensure no precipitation and consequent loss of TA [29]. TA addition was based on the principle of CaO dissolution, whereby the addition of 1 mole of CaO results in a 2-mole increase in TA via bicarbonate (HCO_3^-) formation. To facilitate this process, a highly alkaline solution with a ΔTA of 4000 µmol kg^{-1} was prepared in filtered seawater and subsequently added to the OAE containers.

Nutrient manipulation was confirmed by measurements taken at the start of the experiment (t0). The EN treatment had elevated concentrations of phosphate (3.48 µM) and nitrate (80.77 µM), while the NN treatment reflected background conditions, with only 0.24 µM phosphate and 7.91 µM nitrate (Table 1). Silica concentrations were similar across all treatments, ranging from 44 to 48 µM. These values are consistent with those observed in the Negrito Bay transect (Supplementary Figure S1).

Finally, after all experimental conditions were established, the study was conducted in microcosms (1 L bottles) without airspace. Four experimental conditions were established in a 2 × 2 design, combining two nutrient settings (NN and EN) with two alkalinity conditions (ambient and OAE), with triplicates for each condition and sacrificial sampling at two points, day 3 (t3) and day 6 (t6), resulting in a total of 24 bottles. Among these, the NN + ambient treatment was left unaltered, with no nutrient addition and no alkalinization, and thus represents the closest approximation to a control. The sampling points t3 and t6 were selected based on their relevance to community dynamics. Bottles were incubated in a climate-controlled chamber under conditions matching those recorded at the collection site (18 °C, 150 ± 10 µmol m^{-2} s^{-1} light intensity, and a 14:10 light/dark cycle). To minimize experimental bias, bottles were manually mixed and their position changed twice a day.

2.3. Parameters Evaluated

Carbonate system parameters were sampled at t0, t3 and t6, with TA samples being syringe filtered (polyethersulfone 0.2 µm pore) prior to analysis and measured with Metrohm Titrino Plus 848 coupled with an 869 Compact Sample Changer. Final TA values were corrected against certified reference material supplied by Dickson [30]. Total pH (pH_t) was assessed by glass electrode (WTW, pH 340i) and corrected by TRIS buffer supplied by Dickson [30]. Lastly, pCO_2 and additional components of carbonate chemistry were calculated through the CO2SYS script for excel [31], with salinity, pressure, temperature, total phosphorus and silica, TA, and pHt as input alongside the equilibrium constants defined by Lueker [32].

For dissolved inorganic nutrients determination (nitrate, nitrite, phosphate and silicate), samples were collected on t0, t3 and t6 filtered as described above through a 0.2 µm syringe filter and stored at −20 °C until further analysis. Inorganic nutrients were then determined by spectrophotometry (Varian Cary 50) according to Hansen & Koroleff, (1999) [33] and the concentrations obtained from a calibration curve for each nutrient. The precision for dissolved inorganic phosphate is ±0.02 µmol L^{-1}, for nitrite is ±0.02 µmol L^{-1}, nitrate is ±0.1 µmol L^{-1} and for silicate the precision is ±4% for low values (4.5 µmol L^{-1}), ±2.5% for intermediate values (45 µmol L^{-1}) and ±6% for high values (100 µmol L^{-1}).

Extracellular enzymatic activity of leucine aminopeptidase (LAP) and alkaline phosphatase (ALP) was determined by fluorometric assay based on Hoppe (1983) [34]. The fluorogenic substrate analogs L-leucine-7-amido-4-methylcoumarin hydrochloride (Leu-MCA) for LAP and 4-methylumbelliferyl phosphate (MUF-Phos) for ALP were used. Each substrate was added to 300 µL of sample in black 96-well plates to a final concentration of 32 µM. Samples were incubated in the dark for 3 h at room temperature, and fluorescence was then measured using a FLUOstar Omega microplate reader (BMG LABTECH, Ortenberg, Germany). The values obtained were then assessed using a calibration curve using as standards L-Leucine 7-amido-4-methylcoumarin hydrochloride and 4-Methylumbelliferyl for LAP and ALP, respectively. For alkaline phosphatase samples and standards, 30 µL of ammonia-glycine buffer (final pH 10.5, adjusted with NaOH) was added before readings.

The abundance and composition of microphytoplankton (>20 µm) was assessed from Lugol-fixed samples (2%) (Utermöhl chamber) through inverted microscopy (Nikon TS100, Nikon Corporation, Tokyo, Japan) at 200 × magnification, on t0, t3 and t6. Additional samples were collected to determine the presence of calcifying nanoplankton, specifically coccolithophores. Samples were taken at t0 and t6, filtered onto cellulose nitrate membrane filters, washed with low-mineral water, air-dried, and cut at an angle of approximately 30°. The filter pieces were then mounted on glass slides and fixed with Entellan mounting medium. Coccolithophores were visually identified using a polarization microscope (Leica DM 2700 P, Leica Microsystems, Wetzlar, Germany).

Lastly, the composition of the bacterial community was analyzed using 16S rRNA gene metagenomics. Community samples (approximately 90–150 mL) were collected by vacuum filtration onto 0.22 µm polycarbonate filters (47 mm diameter), which were preserved in 100% ethanol at −20 °C. Prior to DNA extraction, the filters were cut into small pieces. DNA was extracted using the FastDNA™ Spin Kit for Soil (MP Biomedicals, Irvine, CA, USA), following the manufacturer's protocol. The resulting DNA samples were sent to STABVIDA (Lisbon) for paired-end sequencing of the 16S rRNA gene on the Illumina MiSeq platform, targeting the V4 region [35] with primers 515F (5′–3′: GTGCCAGCMGCCGCGGTAA) and 806R (5′–3′: GGACTACHVGGGTWTCTAAT).

2.4. Data Analysis

All statistical analyses were performed using RStudio (V2025.05.0, Boston, MA, USA) [36]. A multifactorial ANOVA was conducted with nutrient treatment and alkalinity treatments as factors, applied to carbonate chemistry parameters, microphytoplankton abundance and enzymatic activity. Post hoc comparisons were performed using Tukey's multiple pairwise comparison test with a 95% confidence interval. Pearson correlation analysis was conducted to evaluate the strength and direction of linear relationships between pairs of continuous variables. For the microphytoplankton community, a PERMANOVA based on Bray–Curtis dissimilarities of Hellinger-transformed abundances was conducted using the vegan package to assess the effects of OAE and/or nutrient treatment.

For the sequencing data, algorithms in QIIME2 (V2023.5, Boulder, CO, USA) were used to transform the amplicon libraries to an amplicon sequence variant (ASV) abundance table. Taxonomy was assigned to ASVs using the SILVA database of the 16S reference sequences at 99% similarity (version 138, released December 2019). While the bacterial community, alpha diversity indexes were calculated using vegan package.

Differences among alpha diversity indexes (Shannon H', Pielou J (evenness) and Fisher alpha (richness)) were determined by a multifactorial ANOVA. The significant effects of OAE within nutrient treatment was assessed through PERMANOVA. A taxon-specific analysis for all relevant orders (relative abundance > 2.5%) was performed through a multifactorial ANOVA applied to general linearized model (GLM) (vegan).

3. Results

3.1. Carbonate Chemistry and Nutrient Conditions

Alkalinity increased consistently across all OAE treatments (Table 2), with comparable magnitudes observed between treatments: TA increased by 177 µmol kg^{-1} in the NN treatment and 170 µmol kg^{-1} in the EN treatment. Thereafter, TA remained stable throughout the duration of the experiment. This initial increase in TA was accompanied by increases in total pH of 0.23 (NN) and 0.25 (EN), as well as decreases in pCO_2 of 182 µatm and 201 µatm, respectively.

Table 2. Carbonate chemistry parameters measured throughout the experiment across all treatments. Values are presented as means with standard errors in parentheses. Sample sizes: T0, n = 1; T3 and T6, n = 3.

		TA (µmol kg^{-1})			**pH_t**			**pCO_2 (µatm)**			**HCO_3^- (µmol kg^{-1})**		
Nutrients	**Alkalinity**	**T0**	**T3**	**T6**	**T0**	**T3**	**T6**	**T0**	**T3**	**T6**	**T0**	**T3**	**T6**
NN	Ambient	2353 (0)	2344 (0.89)	2359 (1.78)	8.05 (0)	8.05 (0)	8.28 (0.06)	409 (0)	399 (2.36)	219 (37.99)	1915 (0)	1901 (5.82)	1696 (2.33)
	OAE	2530 (0)	2516 (1.39)	2528 (0.74)	8.28 (0)	8.22 (0)	8.25 (0)	227 (0)	267 (0.56)	253 (3.30)	1824 (0)	1880 (1.65)	1865 (4.75)
EN	Ambient	2353 (0)	2332 (2.25)	2406 (3.09)	8.03 (0)	8.01 (0)	8.68 (0.03)	429 (0)	445 (1.65)	60 (5.36)	1928 (0)	1923 (0.89)	1211 (38.53)
	OAE	2524 (0)	2505 (1.73)	2537 (7.20)	8.28 (0)	8.24 (0.01)	8.71 (0)	228 (0)	257 (3.73)	57 (0.18)	1820 (0)	1855 (2.35)	1243 (59.47)

The two nutrient regimes exhibited clearly contrasting nutrient drawdown patterns (Figure 2). In the NN treatment, initial phosphate concentrations were low (~0.21 µM) and rapidly depleted, with a 65–68% reduction by day 3. In contrast, the EN treatment started with substantially higher phosphate (~3.5 µM), and concentrations remained near initial levels (0–7% drawdown) by day 3. Nitrate followed a similar trend: in the NN treatment, concentrations declined from ~8 µM to 4–7 µM by day 3 (20–47% drawdown),

whereas in the EN treatment they decreased only slightly (5–12%). Under both regimes, nutrient drawdown was approximately two-fold higher in OAE treatments relative to ambient on day 3. By day 6, nitrate was nearly exhausted across all conditions (86–96% drawdown), while phosphate was reduced to near or below detection. Silicate remained comparatively available, declining only gradually and not becoming limiting during the experiment (Figure 2c).

3.2. Phytoplankton Dynamics

The initial community abundance of 23 cells mL^{-1} increased a noticeable 6- to 9-fold from incubation until the middle of the experiment (Figure 3). By the end of the experiment, phytoplankton abundance differed significantly across treatments, with higher cell numbers in the higher nutrient treatment (Figure 3). Importantly, independent of the nutrient concentrations, there was an OAE effect, decreasing the phytoplankton abundance until day 6, when all treatments showed phosphate depletion (Figures 3 and 2b).

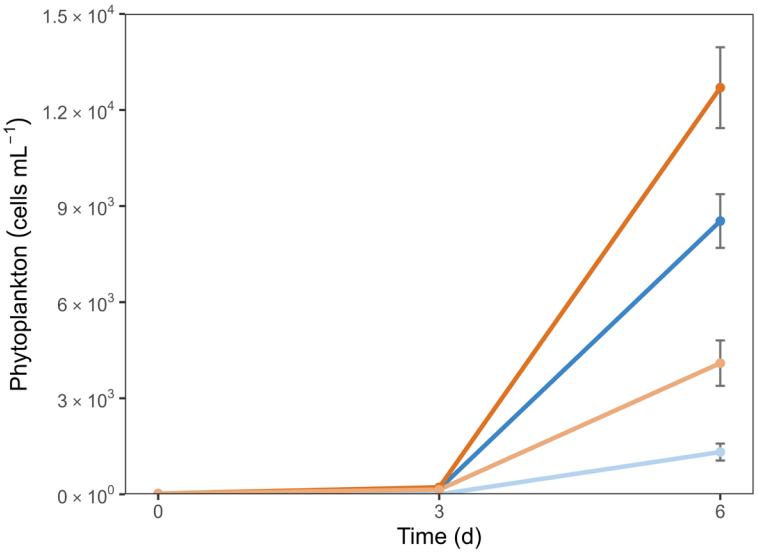

Figure 3. Phytoplankton abundance throughout the experiment. Line colors indicate alkalinity conditions: orange for ambient and blue for OAE. Line shading reflects nutrient treatment: lighter lines show natural nutrients (NN), while darker lines indicate enhanced nutrients (EN).

This pattern was reflected in the fold-change dynamics. Under EN conditions, ambient alkalinity treatments showed a 552-fold increase in abundance by day 6, while OAE treatments increased by only 371-fold. Under natural nutrient (NN) conditions, ambient treatments increased 178-fold, compared to 57-fold under OAE. These results indicate that both nutrient availability ($p < 0.001$) and OAE ($p = 0.003$) had significant effects on phytoplankton abundance, with the influence of OAE evident under both nutrient regimes.

Initially, the phytoplankton community (Figure 4) consisted of approximately 40% coccolithophores, 35% diatoms, 12% dinoflagellates, and 13% unidentified taxa. Over the course of the experiment, a pronounced shift occurred, with diatoms becoming dominant (92–98%) and dinoflagellates comprising 1–9% across all treatments with no statistically significant effects of alkalinity (PERMANOVA, $p = 0.302$) or nutrient enrichment (PERMANOVA, $p = 0.132$), on community composition. This shift was accompanied by a marked decline in dissolved silica concentrations by day 6 (Figure 2c).

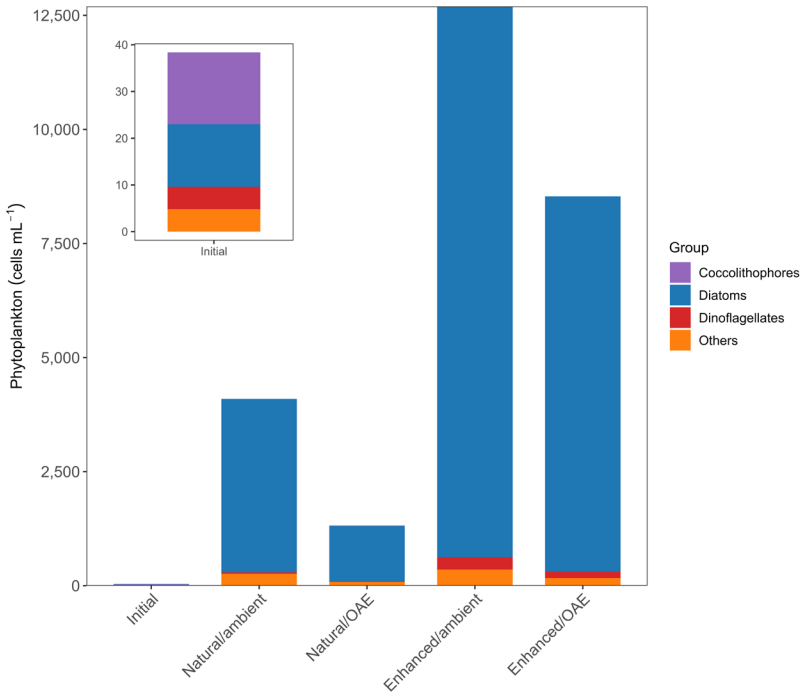

Figure 4. Abundance of phytoplankton functional groups (cells mL^{-1}) in the total community at initial conditions (day 0) and after 6 days under different treatments combining nutrient levels and alkalinity. Treatments include natural or enhanced nutrients and ambient or OAE alkalinity conditions.

3.3. Enzymatic Activity

The activity of leucine aminopeptidase (LAP) was undetectable at t0 and showed similar activity across all treatments mid-experiment (159–205 nmol L^{-1} h^{-1}), indicating no nutrient or OAE effect at that stage. However, by the end of the experiment LAP increased 10-fold under the EN setting (Figure 5a) compared to the NN treatment ($p < 0.001$). Furthermore, under the EN scenario OAE reduced LAP relative to the ambient alkalinity treatment ($p = 0.014$).

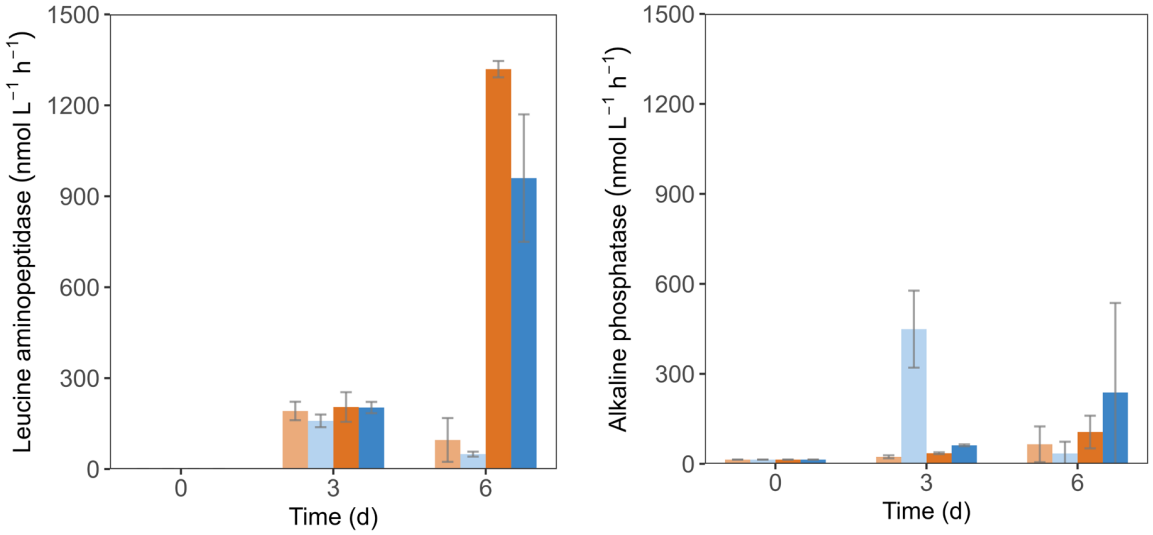

(**a**) (**b**)

Figure 5. Activity rates of: (**a**) leucine aminopeptidase; (**b**) alkaline phosphatase. Bar colors indicate alkalinity conditions: orange for ambient alkalinity and blue for OAE. Line shading reflects nutrient

treatment: lighter lines show natural nutrients (NN), while darker lines indicate enhanced nutrients (EN). Enzyme activity at t0 was below detection. Detection sensitivity was determined by fluorometer resolution and blank variability.

LAP activity showed a strong positive correlation with phytoplankton abundance ($r = 0.93$, $p < 0.001$), supporting a link between phytoplankton biomass and bacterial enzyme activity.

Alkaline phosphatase activity was undetectable at the start of the experiment but peaked by day 3 in the NN treatment under OAE, reaching higher levels (average of 449 nmol L^{-1} h^{-1}) than in all other treatments (23–62 nmol L^{-1} h^{-1}) (Figure 5b). By day 6, however, no significant differences were observed among treatments, despite lower phosphate concentrations in all treatments (Figure 2b).

3.4. Bacterioplankton Community Structure

Bacterial communities across all treatments were dominated by Proteobacteria, primarily Alteromonadales, Oceanospirillales, and Rhodobacterales, and by Bacteroidota, mainly represented by Flavobacteriales (Figure 6). Alpha diversity analysis revealed treatment-specific effects: evenness was slightly reduced in the OAE treatments ($p < 0.047$), while richness significantly declined under enhanced nutrient conditions ($p < 0.01$), as indicated by multifactorial ANOVA.

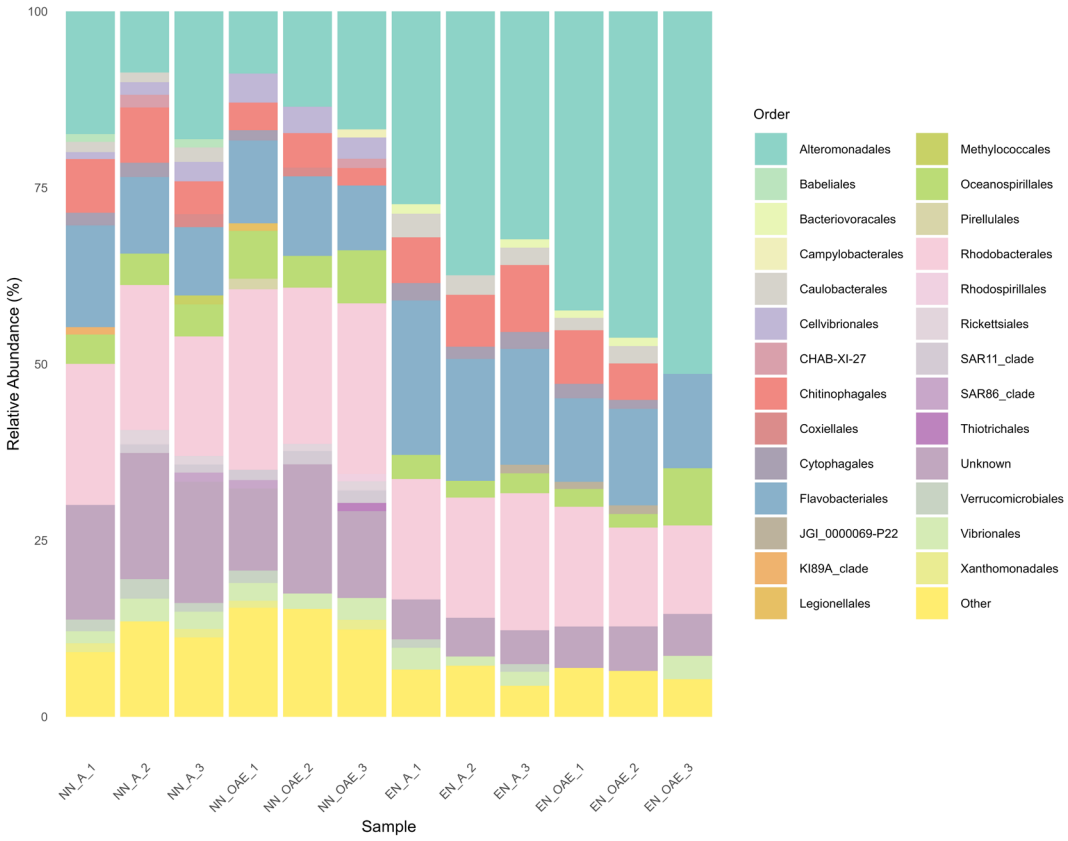

Figure 6. Relative abundance of the 20 most abundant orders in the overall dataset. NN- natural nutrients; EN- enhanced nutrients; A—Ambient alkalinity; OAE—OAE.

Concerning bacterial community composition, no significant effect of OAE was inferred, but instead a significant influence of nutrient enrichment was observed (PERMANOVA; $p = 0.002$). This pattern was held when communities were analyzed separately within each nutrient condition, with OAE continuing to show no significant impact.

Although no overall significant effect of alkalinity on the community composition could be detected, specific microbial orders responded significantly to OAE within each nutrient treatment.

For instance, Chitinophagales, primarily composed of ASVs from the Saprospiraceae family, showed a marked decrease in relative abundance under OAE on both nutrient conditions (Table 3). In the NN condition, Cellvibrionales, composed mainly by the families Halieaceae, Spongiibacteraceae, Porticoccaceae and Cellvibrionaceae exhibited increased relative abundances in response to OAE (Table 3). In the EN condition, both Rhodobacterales (mosly Rhodobacteraceae) and Flavobacteriales (mainly Flavobacteriaceae) decreased in relative abundance under OAE compared to ambient alkalinity (Table 3).

Table 3. GLM results (ANOVA F-tests) showing the effect of OAE on the relative abundance of dominant bacterial orders (>2.5% mean abundance) under natural (NN) and enhanced (EN) nutrient conditions. Significant *p*-values ($p < 0.05$) are shown in bold. Arrows indicate direction of change (↑ increase, ↓ decrease).

Orders	NN *p*-Value	EN *p*-Value	Effect of OAE
Oceanospirillales	0.229	0.798	–
Flavobacteriales	0.764	**0.002**	↓ under EN
Vibrionales	0.918	–	–
Chitinophagales	**0.018**	**0.007**	↓ under NN and EN
Alteromonadales	0.718	0.528	–
Cellvibrionales	**0.026**	–	↑ under NN
Rhodobacterales	0.194	**0.0391**	↓ under EN

Correlations between phytoplankton abundance and the relative abundance of dominant bacterial orders revealed that Chitinophagales had a moderate, non-significant positive association with phytoplankton (r = 0.54, $p = 0.067$), which became significant after excluding an outlier (replicate 3 from the EN + OAE treatment, where Chitinophagales were absent; r = 0.76, $p = 0.006$). Flavobacteriales showed a significant positive correlation with phytoplankton abundance (r = 0.77, $p = 0.003$), whereas Cellvibrionales were negatively associated (r = –0.83, $p < 0.0019$). Rhodobacterales showed no significant relationship to phytoplankton (r = –0.079, $p = 0.807$).

4. Discussion

4.1. Drivers of Phytoplankton Response to Ocean Alkalinity Enhancement

The shift towards diatom dominance in the phytoplankton community was expected under both nutrient conditions, given the initially high concentrations of nitrate, phosphate, and silica that favor rapid diatom growth [37]. While OAE had no significant impact on the overall community composition, it consistently showed lower diatom abundance at the end of the incubation in both enhanced and natural nutrient scenarios. This difference in abundance aligns with previous observations of decreased phytoplankton development under OAE in a similarly non-CO_2-equilibrated experiment [38], and is further supported here by phytoplankton abundance and the OAE induced initial decrease in pCO_2, suggesting that CO_2 limitation likely contributed to the decreased bloom progression, particularly in diatoms.

Moreover, the decrease in phytoplankton abundance regardless of the nutrient condition reported is a novel observation. However, previous non-equilibrated, calcium-based OAE experiments have documented delays in phytoplankton blooms [39]. This could raise the possibility that, rather than a true decline in biomass, we might have observed a delay in phytoplankton development. Yet, the clear nutrient drawdown observed (Figure 2a–c), particularly phosphate depletion, suggests that the communities had already undergone

active growth, supporting that we observed an actual reduction in abundance rather than a delayed bloom. To cope with potential CO_2 limitation under these conditions, diatoms likely relied on carbon-concentrating mechanisms (CCMs) to enhance the efficiency of RubisCO [40,41]. While CCMs do not consume inorganic phosphate (Pi) directly, Pi is indirectly essential for the energy and metabolic processes required to sustain their operation. Furthermore, recent laboratory studies have demonstrated reduced growth rates in *Thalassiosira pseudonana* under prolonged alkalinization without CO_2 replenishment [42], reinforcing the idea that elevated alkalinity and limited pCO_2 can directly constrain phytoplankton growth.

Conversely, lab experiments using CO_2-equilibrated conditions reported no change in *Chaetoceros* sp. growth [43] and other non-equilibrated OAE studies with higher TA increases (~300–500 µmol kg^{-1}) also found no decrease in phytoplankton abundance [20,22]. Nevertheless, those studies differed in both carbonate chemistry and nutrient conditions, suggesting that microbial responses to OAE are context-dependent and likely shaped by site-specific environmental settings.

It is important to note that while we observed consistent reductions in phytoplankton abundance under OAE conditions, direct measurements of biomass (e.g., chlorophyll *a* or particulate organic carbon) were not conducted. Thus, while our data strongly indicates a suppression of phytoplankton development, particularly among diatoms, we cannot rule out the possibility of size-structure shifts that could influence total biomass. However, the strong nutrient drawdown observed across treatments, especially phosphate, suggests that the communities experienced active growth rather than delayed development, lending support to the interpretation of a real decline in population-level productivity.

These results highlight that OAE can alter bloom progression even when nutrients are not limiting. The consistent reduction in diatom abundance across both nutrient regimes suggests that OAE effects extend beyond nutrient availability and may influence phytoplankton community development under different environmental settings.

4.2. Phytoplankton-Mediated Enzymatic Activity Under Ocean Alkalinity Enhancement

Concomitantly with the increase in phytoplankton abundance, LAP activity increased significantly under nutrient enrichment by the end of the experiment. While this pattern suggests elevated enzymatic activity during the bloom, it is important to note that the LAP measured here reflects extracellular enzyme activity, which is primarily of bacterial origin. Therefore, the increase in LAP is likely a microbial response to enhanced organic substrate availability from the blooming phytoplankton—particularly leucine-rich compounds commonly released during diatom blooms [44]. This interpretation is consistent with the dominance of diatoms in the phytoplankton community and the co-occurrence of diatom-associated bacterial taxa such as Flavobacteriaceae and Saprospiraceae, both known for degrading high-molecular-weight organic matter [45–47]. While LAP activity was lower under OAE in the EN setting, this difference was not observed when normalized to phytoplankton abundance. This suggests that the OAE-driven reduction in LAP activity was not a direct effect on bacterial enzymatic function, but instead mediated by lower phytoplankton biomass and, by extension, reduced substrate availability. The potential mechanisms underlying this phytoplankton–bacteria coupling, including changes in bacterial community structure and the role of diatom-associated taxa, are explored further in Section 4.3.

The transient increase in ALP activity under OAE in the natural nutrient (NN) setting coincided with early phosphate depletion (Figures 2b and 5b), consistent with ALP's role in mobilizing phosphorus under limiting conditions [48]. By the end of the experiment, phosphate was depleted across all treatments, and no differences in ALP activity were

detected between OAE and control groups or between nutrient regimes. These results could indicate that the observed ALP response to OAE was not a direct effect of alkalinity enhancement, but rather indirectly driven by changes in microbial community structure during early phosphorus stress.

4.3. Phytoplankton–Bacteria Coupling Shapes Microbial Responses to OAE

The relative abundance of Flavobacteriaceae and Saprospiraceae was positively correlated with phytoplankton abundance, while Cellvibrionales were inversely correlated, indicating that their responses were not directly driven by the changes in carbonate system that result of OAE, but instead mediated through changes in phytoplankton abundance. Since phytoplankton abundance was sensitive to both nutrient enrichment and OAE—particularly the decreased diatom bloom under OAE—shifts in these bacterial groups could reflect changes in organic matter availability linked to bloom development. These findings are consistent with the ecological roles of both taxa: Saprospiraceae are commonly epiphytic and associated with algae, particles, and filamentous bacteria [47,49,50], while Flavobacteriaceae are frequently linked to diatom blooms and known for degrading high-molecular-weight organic compounds [51]. In contrast, the negative correlation of Cellvibrionales with phytoplankton abundance suggests an earlier role in bloom succession, consistent with findings from upwelling systems where Cellvibrionales dominate during bloom initiation, while Flavobacteriales and Saprospirales become more prominent during bloom decay and senescence as DOM composition shifts [52]. Rhodobacteraceae showed reduced relative abundance under OAE but only in the enhanced nutrient setting, a response likely linked to shifts in phytoplankton dynamics. As phytoplankton succession and the composition of associated dissolved organic matter (DOM) are major factors shaping bacterioplankton communities [52–54], the abundance in bloom progression under OAE likely influenced substrate availability and timing, altering conditions for Rhodobacteraceae proliferation.

These patterns highlight the close ecological coupling between bacterioplankton and phytoplankton, which supply essential organic substrates and nutrients that support bacterial growth and activity [55–58]. This tight interdependence helps explain the observed correlations between specific bacterial taxa and phytoplankton abundance. Perturbations to marine biogeochemistry, such as elevated CO_2 levels and ocean alkalinity enhancement (OAE), can therefore indirectly shape bacterioplankton community composition and function by altering phytoplankton bloom dynamics and the quantity and quality of available organic matter [59–63].

Taken together, our findings suggest that microbial ecosystem responses to OAE are strongly mediated by nutrient context and phytoplankton–bacteria coupling. This indicates that the ecological consequences of large-scale OAE deployment are unlikely to be uniform across environments and should be evaluated within the framework of site-specific nutrient regimes and microbial dynamics.

5. Conclusions

Our results show that OAE consistently reduced diatom development across contrasting nutrient conditions, leading to reduced phytoplankton-derived organic matter and downstream effects on microbial enzymatic activity and bacterioplankton composition. These findings demonstrate that the ecological consequences of OAE are not limited to carbonate chemistry alone but are influenced by nutrient availability and phytoplankton–bacteria coupling.

From a broader perspective, this suggests that OAE deployment could alter microbial ecosystem functioning in ways that are both nutrient-dependent and context-specific. A

consistent reduction in phytoplankton biomass under OAE conditions raises the possibility of locally diminished primary productivity, with implications for microbial food web dynamics. While our study was limited to short-term incubations, it underscores the importance of integrating microbial responses into assessments of OAE feasibility and considering baseline nutrient conditions when evaluating its ecological consequences.

Supplementary Materials: The following supporting information can be downloaded at: https://www.mdpi.com/article/10.3390/oceans6040065/s1, Figure S1: Inorganic nutrient concentrations at sampling sites A, B, C, D and E (Negrito Bay).

Author Contributions: Conceptualization and experimental design: I.d.C. and J.B.e.R. Investigation and data analysis: I.d.C., J.B.e.R., S.C.R., P.F.S.B., M.C. and A.L. Funding acquisition: J.B.e.R. and E.B.d.A. Writing of original draft: I.d.C. Reviewing and editing of original draft: I.d.C., S.C.R., A.L., N.C.M.G., M.C., P.F.S.B., E.B.d.A. and J.B.e.R. All authors have read and agreed to the published version of the manuscript.

Funding: This research was supported by the FCT project of IITAA with the reference UIDB/00153/2020, by the ARM Program supported by DOE, in the framework of the ENA project through the agreement between LANL and the University of the Azores, IC is financed by National Funds through the Portuguese funding agency, FCT -Fundação para a Ciência e a Tecnologia with the grant UI/BD/150890/2021, SCR is supported by FCT grant UIDP/00153/2020, and JBR is supported by FCT, within Contrato-Programa, Apoio Institucional.

Data Availability Statement: The original contributions presented in this study are included in the article. Further inquiries can be directed to the corresponding author.

Conflicts of Interest: The authors declare no conflicts of interest.

Abbreviations

The following abbreviations are used in this manuscript:

ALP	Alkaline phosphatase
CCM	Carbon-concentrating mechanism
LAP	Leucine aminopeptidase
OAE	Ocean Alkalinity Enhancement
TA	Total Alkalinity

References

1. *United Nations Framework Convention on Climate Change Paris Agreement*; United Nations: New York, NY, USA, 2015.
2. Calvin, K.; Dasgupta, D.; Krinner, G.; Mukherji, A.; Thorne, P.W.; Trisos, C.; Romero, J.; Aldunce, P.; Barrett, K.; Blanco, G.; et al. *IPCC, 2023: Climate Change 2023: Synthesis Report, Contribution of Working Groups I, II and III to the Sixth Assessment Report of the Intergovernmental Panel on Climate Change*; Core Writing Team, Lee, H., Romero, J., Eds.; IPCC: Geneva, Switzerland, 2023.
3. Low, S.; Baum, C.M.; Sovacool, B.K. Rethinking Net-Zero Systems, Spaces, and Societies: "Hard" versus "Soft" Alternatives for Nature-Based and Engineered Carbon Removal. *Glob. Environ. Change* **2022**, *75*, 102530. [CrossRef]
4. Rau, G.H.; McLeod, E.L.; Hoegh-Guldberg, O. The Need for New Ocean Conservation Strategies in a High-Carbon Dioxide World. *Nat. Clim. Chang.* **2012**, *2*, 720–724. [CrossRef]
5. Bach, L.T.; Gill, S.J.; Rickaby, R.E.M.; Gore, S.; Renforth, P. CO_2 Removal with Enhanced Weathering and Ocean Alkalinity Enhancement: Potential Risks and Co-Benefits for Marine Pelagic Ecosystems. *Front. Clim.* **2019**, *1*, 7. [CrossRef]
6. Gattuso, J.-P.; Williamson, P.; Duarte, C.M.; Magnan, A.K. The Potential for Ocean-Based Climate Action: Negative Emissions Technologies and Beyond. *Front. Clim.* **2021**, *2*, 575716. [CrossRef]
7. Hartmann, J.; West, A.J.; Renforth, P.; Köhler, P.; De La Rocha, C.L.; Wolf-Gladrow, D.A.; Dürr, H.H.; Scheffran, J. Enhanced Chemical Weathering as a Geoengineering Strategy to Reduce Atmospheric Carbon Dioxide, Supply Nutrients, and Mitigate Ocean Acidification. *Rev. Geophys.* **2013**, *51*, 113–149. [CrossRef]
8. Kheshgi, H.S. Sequestering Atmospheric Carbon Dioxide by Increasing Ocean Alkalinity. *Energy* **1995**, *20*, 915–922. [CrossRef]
9. Renforth, P.; Henderson, G. Assessing Ocean Alkalinity for Carbon Sequestration. *Rev. Geophys.* **2017**, *55*, 636–674. [CrossRef]

10. Feng, E.Y.; Keller, D.P.; Koeve, W.; Oschlies, A. Could Artificial Ocean Alkalinization Protect Tropical Coral Ecosystems from Ocean Acidification? *Environ. Res. Lett.* **2016**, *11*, 074008. [CrossRef]
11. Gattuso, J.P.; Magnan, A.K.; Bopp, L.; Cheung, W.W.L.; Duarte, C.M.; Hinkel, J.; Mcleod, E.; Micheli, F.; Oschlies, A.; Williamson, P.; et al. Ocean Solutions to Address Climate Change and Its Effects on Marine Ecosystems. *Front. Mar. Sci.* **2018**, *5*, 337. [CrossRef]
12. Keller, D.P.; Feng, E.Y.; Oschlies, A. Potential Climate Engineering Effectiveness and Side Effects during a High Carbon Dioxide-Emission Scenario. *Nat. Commun.* **2014**, *5*, 3304. [CrossRef]
13. Eisaman, M.D.; Geilert, S.; Renforth, P.; Bastianini, L.; Campbell, J.; Dale, A.W.; Foteinis, S.; Grasse, P.; Hawrot, O.; Löscher, C.R.; et al. Assessing the Technical Aspects of Ocean-Alkalinity-Enhancement Approaches. *State Planet.* **2023**, *3*, 2-oae2023. [CrossRef]
14. Foteinis, S.; Andresen, J.; Campo, F.; Caserini, S.; Renforth, P. Life Cycle Assessment of Ocean Liming for Carbon Dioxide Removal from the Atmosphere. *J. Clean. Prod.* **2022**, *370*, 133309. [CrossRef]
15. Renforth, P.; Jenkins, B.G.; Kruger, T. Engineering Challenges of Ocean Liming. *Energy* **2013**, *60*, 442–452. [CrossRef]
16. Marín-Samper, L.; Arístegui, J.; Hernández-Hernández, N.; Ortiz, J.; Archer, S.D.; Ludwig, A.; Riebesell, U. Assessing the Impact of CO_2-Equilibrated Ocean Alkalinity Enhancement on Microbial Metabolic Rates in an Oligotrophic System. *Biogeosciences* **2024**, *21*, 2859–2876. [CrossRef]
17. Ramírez, L.; Pozzo-Pirotta, L.J.; Trebec, A.; Manzanares-Vázquez, V.; Díez, J.L.; Arístegui, J.; Riebesell, U.; Archer, S.D.; Segovia, M. Ocean Alkalinity Enhancement (OAE) Does Not Cause Cellular Stress in a Phytoplankton Community of the Subtropical Atlantic Ocean. *Biogeosciences* **2025**, *22*, 1865–1886. [CrossRef]
18. Subhas, A.V.; Marx, L.; Reynolds, S.; Flohr, A.; Mawji, E.W.; Brown, P.J.; Cael, B.B. Microbial Ecosystem Responses to Alkalinity Enhancement in the North Atlantic Subtropical Gyre. *Front. Clim.* **2022**, *4*, 784997. [CrossRef]
19. Suessle, P.; Taucher, J.; Goldenberg, S.U.; Baumann, M.; Spilling, K.; Noche-Ferreira, A.; Vanharanta, M.; Riebesell, U. Particle Fluxes by Subtropical Pelagic Communities under Ocean Alkalinity Enhancement. *Biogeosciences* **2025**, *22*, 71–86. [CrossRef]
20. Guo, J.A.; Strzepek, R.F.; Swadling, K.M.; Townsend, A.T.; Bach, L.T. Influence of Ocean Alkalinity Enhancement with Olivine or Steel Slag on a Coastal Plankton Community in Tasmania. *Biogeosciences* **2024**, *21*, 2335–2354. [CrossRef]
21. Guo, J.A.; Strzepek, R.F.; Yuan, Z.; Swadling, K.M.; Townsend, A.T.; Achterberg, E.P.; Browning, T.J.; Bach, L.T. Effects of Ocean Alkalinity Enhancement on Plankton in the Equatorial Pacific. *Commun. Earth Env.* **2025**, *6*, 270. [CrossRef]
22. Ferderer, A.; Chase, Z.; Kennedy, F.; Schulz, K.G.; Bach, L.T. Assessing the Influence of Ocean Alkalinity Enhancement on a Coastal Phytoplankton Community. *Biogeosciences* **2022**, *19*, 5375–5399. [CrossRef]
23. Xin, X.; Goldenberg, S.U.; Taucher, J.; Stuhr, A.; Arístegui, J.; Riebesell, U. Resilience of Phytoplankton and Microzooplankton Communities under Ocean Alkalinity Enhancement in the Oligotrophic Ocean. *Env. Sci. Technol.* **2024**, *58*, 20918–20930. [CrossRef]
24. Barcelos e Ramos, J.; Schulz, K.G.; Voss, M.; Narciso, Á.; Müller, M.N.; Reis, F.V.; Cachão, M.; Azevedo, E.B. Nutrient-Specific Responses of a Phytoplankton Community: A Case Study of the North Atlantic Gyre, Azores. *J. Plankton Res.* **2017**, *39*, 744–761. [CrossRef]
25. Crummett, L.T. Acidification Decreases Microbial Community Diversity in the Salish Sea, a Region with Naturally High pCO_2. *PLoS ONE* **2020**, *15*, e0241183. [CrossRef] [PubMed]
26. Lin, S. Phosphate Limitation and Ocean Acidification Co-Shape Phytoplankton Physiology and Community Structure. *Nat. Commun.* **2023**, *14*, 2699. [CrossRef] [PubMed]
27. Burt, D.J.; Fröb, F.; Ilyina, T. The Sensitivity of the Marine Carbonate System to Regional Ocean Alkalinity Enhancement. *Front. Clim.* **2021**, *3*, 624075. [CrossRef]
28. Jürchott, M.; Oschlies, A.; Koeve, W. Artificial Upwelling—A Refined Narrative. *Geophys. Res. Lett.* **2023**, *50*, e2022GL101870. [CrossRef]
29. Moras, C.A.; Bach, L.T.; Cyronak, T.; Joannes-Boyau, R.; Schulz, K.G. Ocean Alkalinity Enhancement—Avoiding Runaway CaCO3 Precipitation during Quick and Hydrated Lime Dissolution. *Biogeosciences* **2022**, *19*, 3537–3557. [CrossRef]
30. Dickson, A.G.; Afghan, J.D.; Anderson, G.C. Reference Materials for Oceanic CO_2 Analysis: A Method for the Certification of Total Alkalinity. *Mar. Chem.* **2003**, *80*, 185–197. [CrossRef]
31. Lewis, E.; Wallace, D.; Allison, L.J. *Program Developed for CO_2 System Calculations*; Oak Ridge National Laboratory: Oak Ridge, TN, USA, 1998.
32. Lueker, T.J.; Dickson, A.G.; Keeling, C.D. Ocean PCO Calculated from Dissolved Inorganic Carbon, 2 Alkalinity, and Equations for K and K: Validation Based on 1 2 Laboratory Measurements of CO in Gas and Seawater at 2 Equilibrium. *Mar. Chem.* **2000**, *70*, 105–119. [CrossRef]
33. Hansen, H.; Koroleff, F. Determination of Nutrients. In *Methods of Seawater Analysis*; Wiley: Hoboken, NJ, USA, 1999.
34. Hoppe, H.-G. Significance of Exoenzymatic Activities in the Ecology of Brackish Water: Measurements by Means of Methylumbelliferyl-Substrates. *Mar. Ecol. Prog. Ser.* **1983**, *11*, 299–308. [CrossRef]
35. Caporaso, J.G.; Lauber, C.L.; Walters, W.A.; Berg-Lyons, D.; Lozupone, C.A.; Turnbaugh, P.J.; Fierer, N.; Knight, R. Global Patterns of 16S RRNA Diversity at a Depth of Millions of Sequences per Sample. *Proc. Natl. Acad. Sci. USA* **2011**, *108*, 4516–4522. [CrossRef]
36. Posit Team. *RStudio: Integrated Development Environment for R*, Version 2025.05.0; Posit Software PBC: Boston, MA, USA, 2025.

37. Reynolds, C.S. The Response of Phytoplankton Communities to Changing Lake Environments. *Swiss J. Hydrol.* **1987**, *49*, 220–236. [CrossRef]
38. de Castro, I.; Ribeiro, S.C.; Louvado, A.; Gomes, N.C.M.; Cachão, M.; Brito de Azevedo, E.; Barcelos e Ramos, J. Ocean Liming Effect on a North Atlantic Microbial Community: Changes in Composition and Rates. *Front. Mar. Sci.* **2025**, *12*, 1602158. [CrossRef]
39. Marín-Samper, L.; Arístegui, J.; Hernández-Hernández, N.; Riebesell, U. Responses of Microbial Metabolic Rates to Non-Equilibrated Silicate- versus Calcium-Based Ocean Alkalinity Enhancement. *Biogeosciences* **2024**, *21*, 5707–5724. [CrossRef]
40. Matsuda, Y.; Hopkinson, B.M.; Nakajima, K.; Dupont, C.L.; Tsuji, Y. Mechanisms of Carbon Dioxide Acquisition and CO 2 Sensing in Marine Diatoms: A Gateway to Carbon Metabolism. *Philos. Trans. R. Soc. B Biol. Sci.* **2017**, *372*, 20160403. [CrossRef]
41. Hopkinson, B.M.; Dupont, C.L.; Matsuda, Y. The Physiology and Genetics of CO_2 Concentrating Mechanisms in Model Diatoms. *Curr. Opin. Plant Biol.* **2016**, *31*, 51–57. [CrossRef] [PubMed]
42. Oberlander, J.L.; Burke, M.E.; London, C.A.; Macintyre, H.L. Assessing the Impacts of Simulated Ocean Alkalinity Enhancement on Viability and Growth of Nearshore Species of Phytoplankton. *Biogeosciences* **2025**, *22*, 499–512. [CrossRef]
43. Gately, J.A.; Kim, S.M.; Jin, B.; Brzezinski, M.A.; Iglesias-Rodriguez, M.D. Coccolithophores and Diatoms Resilient to Ocean Alkalinity Enhancement: A Glimpse of Hope? *Sci. Adv.* **2023**, *9*, adg6066. [CrossRef]
44. Shi, Z.; Xu, J.; Li, X.; Li, R.; Li, Q. Links of Extracellular Enzyme Activities, Microbial Metabolism, and Community Composition in the River-Impacted Coastal Waters. *J. Geophys. Res. Biogeosci* **2019**, *124*, 3507–3520. [CrossRef]
45. Buchan, A.; LeCleir, G.R.; Gulvik, C.A.; González, J.M. Master Recyclers: Features and Functions of Bacteria Associated with Phytoplankton Blooms. *Nat. Rev. Microbiol.* **2014**, *12*, 686–698. [CrossRef]
46. McIlroy, S.J.; Nielsen, P.H. The Family Saprospiraceae. In *The Prokaryotes*; Springer: Berlin/Heidelberg, Germany, 2014; pp. 863–889.
47. Xia, Y.; Kong, Y.; Thomsen, T.R.; Halkjær Nielsen, P. Identification and Ecophysiological Characterization of Epiphytic Protein-Hydrolyzing *Saprospiraceae* ("*Candidatus Epiflobacter*" spp.) in Activated Sludge. *Appl. Environ. Microbiol.* **2008**, *74*, 2229–2238. [CrossRef] [PubMed]
48. Hoppe, H.-G. Phosphatase Activity in the Sea. *Hydrobiologia* **2003**, *493*, 187–200. [CrossRef]
49. Korlević, M.; Markovski, M.; Zhao, Z.; Herndl, G.J.; Najdek, M. Seasonal Dynamics of Epiphytic Microbial Communities on Marine Macrophyte Surfaces. *Front. Microbiol.* **2021**, *12*, 671342. [CrossRef]
50. Miranda, L.N.; Hutchison, K.; Grossman, A.R.; Brawley, S.H. Diversity and Abundance of the Bacterial Community of the Red Macroalga Porphyra Umbilicalis: Did Bacterial Farmers Produce Macroalgae? *PLoS ONE* **2013**, *8*, e58269. [CrossRef] [PubMed]
51. Grossart, H.; Levold, F.; Allgaier, M.; Simon, M.; Brinkhoff, T. Marine Diatom Species Harbour Distinct Bacterial Communities. *Env. Microbiol.* **2005**, *7*, 860–873. [CrossRef]
52. Pontiller, B.; Martínez-García, S.; Joglar, V.; Amnebrink, D.; Pérez-Martínez, C.; González, J.M.; Lundin, D.; Fernández, E.; Teira, E.; Pinhassi, J. Rapid Bacterioplankton Transcription Cascades Regulate Organic Matter Utilization during Phytoplankton Bloom Progression in a Coastal Upwelling System. *ISME J.* **2022**, *16*, 2360–2372. [CrossRef]
53. Delgadillo-Nuño, E.; Teira, E.; Pontiller, B.; Lundin, D.; Joglar, V.; Pedrós-Alió, C.; Fernández, E.; Pinhassi, J.; Martínez-García, S. Coastal Upwelling Systems as Dynamic Mosaics of Bacterioplankton Functional Specialization. *Front. Mar. Sci.* **2023**, *10*, 1259783. [CrossRef]
54. Teeling, H.; Fuchs, B.M.; Becher, D.; Klockow, C.; Gardebrecht, A.; Bennke, C.M.; Kassabgy, M.; Huang, S.; Mann, A.J.; Waldmann, J.; et al. Substrate-Controlled Succession of Marine Bacterioplankton Populations Induced by a Phytoplankton Bloom. *Science* **2012**, *336*, 608–611. [CrossRef]
55. Amin, S.A.; Parker, M.S.; Armbrust, E.V. Interactions between Diatoms and Bacteria. *Microbiol. Mol. Biol. Rev.* **2012**, *76*, 667–684. [CrossRef]
56. Eigemann, F.; Rahav, E.; Grossart, H.; Aharonovich, D.; Sher, D.; Vogts, A.; Voss, M. Phytoplankton Exudates Provide Full Nutrition to a Subset of Accompanying Heterotrophic Bacteria via Carbon, Nitrogen and Phosphorus Allocation. *Environ. Microbiol.* **2022**, *24*, 2467–2483. [CrossRef]
57. Kieft, B.; Li, Z.; Bryson, S.; Hettich, R.L.; Pan, C.; Mayali, X.; Mueller, R.S. Phytoplankton Exudates and Lysates Support Distinct Microbial Consortia with Specialized Metabolic and Ecophysiological Traits. *Proc. Natl. Acad. Sci. USA* **2021**, *118*, e2101178118. [CrossRef]
58. Seymour, J.R.; Amin, S.A.; Raina, J.-B.; Stocker, R. Zooming in on the Phycosphere: The Ecological Interface for Phytoplankton–Bacteria Relationships. *Nat. Microbiol.* **2017**, *2*, 17065. [CrossRef]
59. Bunse, C.; Lundin, D.; Karlsson, C.M.G.; Akram, N.; Vila-Costa, M.; Palovaara, J.; Svensson, L.; Holmfeldt, K.; González, J.M.; Calvo, E.; et al. Response of Marine Bacterioplankton PH Homeostasis Gene Expression to Elevated CO_2. *Nat. Clim. Change* **2016**, *6*, 483–487. [CrossRef]

60. Huang, R.; Sun, J.; Yang, Y.; Jiang, X.; Wang, Z.; Song, X.; Wang, T.; Zhang, D.; Li, H.; Yi, X.; et al. Elevated pCO_2 Impedes Succession of Phytoplankton Community from Diatoms to Dinoflagellates Along with Increased Abundance of Viruses and Bacteria. *Front. Mar. Sci.* **2021**, *8*, 642208. [CrossRef]
61. Sperling, M.; Piontek, J.; Gerdts, G.; Wichels, A.; Schunck, H.; Roy, A.-S.; La Roche, J.; Gilbert, J.; Nissimov, J.I.; Bittner, L.; et al. Effect of Elevated CO_2 on the Dynamics of Particle-Attached and Free-Living Bacterioplankton Communities in an Arctic Fjord. *Biogeosciences* **2013**, *10*, 181–191. [CrossRef]
62. Wang, Y.; Zhang, R.; Yang, Y.; Tu, Q.; Zhou, J.; Jiao, N. Ocean Acidification Altered Microbial Functional Potential in the Arctic Ocean. *Limnol. Ocean.* **2023**, *68*, S217–S229. [CrossRef]
63. Xia, X.; Wang, Y.; Yang, Y.; Luo, T.; Van Nostrand, J.D.; Zhou, J.; Jiao, N.; Zhang, R. Ocean Acidification Regulates the Activity, Community Structure, and Functional Potential of Heterotrophic Bacterioplankton in an Oligotrophic Gyre. *J. Geophys. Res. Biogeosci.* **2019**, *124*, 1001–1017. [CrossRef]